DESIGN AND IMPEDANCE OPTIMIZATION OF THE SIRIUS BPM BUTTON

H. O. C. Duarte#, L. Sanfelici, S. R. Marques, LNLS, Campinas, SP, Brazil

Abstract

Design of several BPM Buttons is presented with detail impedance, heat transfer and mechanical analysis. Special attention is given to the application of ceramics as materials with low relative permittivity inside of the BPM Button and to the geometric shape of the BPM Button. The heat dissipation is evaluated based on the loss factor calculated for a 2.65 mm bunch length. The narrow-band impedance is discussed and its dependence on applied ceramic materials is compared.

INTRODUCTION

One of the main concerns in the BPM Button design, especially for the storage rings with short, high-current circulating bunches, is heating due to Higher Order Modes (HOM's) [1]. The BPM Button geometry and the materials choice need to be optimized from impedance and heat transfer points of view to avoid BPM Button overheating due to the resonance modes generated between the housing and the BPM Button itself by a passing bunch [2].

In this paper we discuss the results for three different BPM Button geometries. The main attention has been paid to: 1) The frequency spectrum of HOM's and their electrodynamics parameters, 2) The electrical conductivity of the BPM Button, 3) The thermal conductivity of ceramics materials, 4) The dielectric permittivity of ceramics, 5) Geometric dimensions of the BPM Button and the BPM housing, 6) Manufacturing process of the ceramics and BPM Buttons, 7) The magnitude of the signal out of feed-through at RF frequency of 500 MHz.

IMPEDANCE OPTIMIZATION

In this paper we present three candidates of the BPM Button for the 3GeV Sirius storage ring. The third-generation light source is under construction at LNLS, the Brazilian Synchrotron Light Laboratory. The work has been started from analysis of already existed BPM Button geometries and from their optimization process. Blednykh, Ferreira and Krinsky [2] have shown the possibility of resonance modes suppression due to changes in geometric dimensions of housings for the BPM Button. We were interested in further impedance optimization of the BPM Button geometry and applied different dielectric materials to understand their effect on the broad-band and narrow-band impedances. Several dielectric materials as the vacuum insulator have been considered with high thermal conductivity to provide good heat transfer between the BPM Button and the BPM housing. Aluminum Nitride (AlN) and Boron Nitride (BN) composite materials have been chosen for analysis as shown in Table 1.

#henrique.caiafa@lnls.br

Table 1: Properties of Dielectric Materials for Simulations

Considered Properties	Value (AlN – BN)
Permittivity, ε_r	9 – 4
Thermal Conductivity, σ_t	160 – 46 W/K.m
Loss Tangent, $\tan\delta_\varepsilon$, @1MHz	0.003 – 0.0034

Two geometries, the standard BPM Button and the modified BPM Button are shown in Fig. 1a and in Fig. 1b respectively. The difference between two geometries is in location of the vacuum insulator. In modified BPM geometry (Fig. 1b), the dielectric material lies on top of the button. It helps to improve the heat transfer efficiency. The BPM Button with 6 mm diameter is connected to the inner pin. The pin diameter near the button is optimized based upon the dielectric material to match the characteristic impedance of the feedthrough: 0.54 mm with AlN and 1.24 mm with BN. The gap between the BPM housing and the BPM Button is 0.3 mm. The BPM Button is located on the round vacuum chamber with R = 11.7 mm radius.

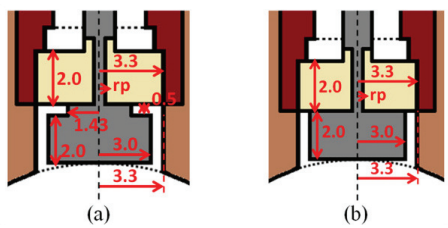

Figure 1: a) The inner profile of the standard BPM Button geometry. b) Modified BPM Button with dielectric material on top of it. All units are in mm.

The GdfidL code has been used for numerical simulations [3]. As can be seen from the results presented in Fig. 2a and Fig. 2b, there are additional resonant modes, which are generated inside the dielectric material by a passing bunch. The dielectric material is seen by the beam and it agrees with that was found for the NSLS-II BPM Button [4]. The electromagnetic fields, excited in dielectric materials, radiate back into the chamber through the tiny gap. The resonant modes in dielectric material have been classified. It is H_{m1p}-Mode as in the coaxial dielectric-filled cavity. The preliminary frequencies of those modes can be found using the following equation

$$f_r^{Hml\,p} = \frac{1}{\sqrt{\varepsilon_r}} \frac{c}{2\pi} \sqrt{\left(\frac{2m}{r_p + r_h}\right)^2 + \left(\frac{\pi p}{t_c}\right)^2} \,. \qquad (1)$$

ISBN 978-3-95450-127-4

where ε_r is the dielectric permittivity and m and p are integers. The integer m is the azimuthal index and p is the longitudinal mode number. The geometry parameters r_p, r_h and t_c are the pin radius (within the insulator), housing radius and ceramics thickness, respectively. Since the electromagnetic fields of those modes can propagate through the gap (modes are not strongly trapped) we would expect some differences between simulated data and the frequencies due to Eq. (1). As an example, the dielectric thickness t_c in Eq. (1) has been fitted to obtain the same frequency as numerically calculated.

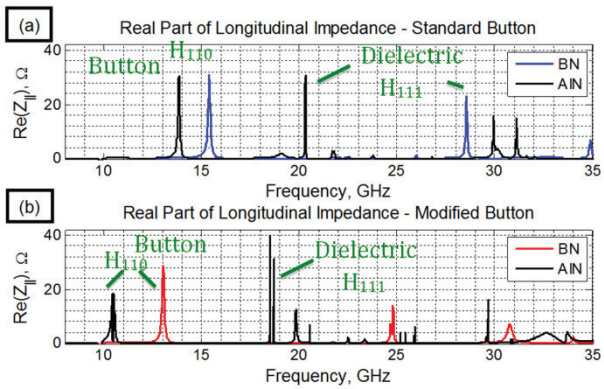

Figure 2: Real part of the longitudinal impedance for: a) Standard BPM Button. b) Modified BPM Button. The frequency axis is shown in frequency range 8 GHz-35 GHz since there are no other modes below 8 GHz.

Frequencies are in a good agreement for the standard BPM Button if t_c is taken as 2.5 mm vs. 2 mm originally used. Frequencies of H_{111}-Mode due to Eq. (1) with t_c = 2.5 mm are f = 20.6 GHz for AlN and f = 30.9 GHz for BN, which is still above the frequency numerically obtained, $f_{BN,\,H111}$ = 28.5 GHz. The frequency spectrum of the modified BPM Button looks different from the standard one, since the dielectric material is located right on top of the button (Fig. 1b) and there is no additional gap between the dielectric material and the button surface. In this case the frequencies of H_{111}-Mode are f_{AlN} = 18.3GHz and f_{BN} = 25 GHz.

For the thin BPM Buttons without dielectric material, frequencies of the trapped modes, generated between the BPM housing and the button itself, can be defined as

$$f_c^{Hml} = \frac{c}{\pi}\frac{m}{r_b + r_h}. \qquad (2)$$

where r_b is the button radius. The frequency of H_{11}-Mode (f_{H11}~$f_{c,H11}$) is 15.2 GHz for geometric parameters specified in Fig 1. As can be seen from Fig. 2a, the frequency of the trapped mode due to the button geometry is shifted down in frequency scale. It happened because of dielectric material (AlN) in the geometry with high dielectric constant ε_r = 9 (black curve). In the case of BN with ε_r = 4, the frequency of H_{110}-mode does not change significantly and remains as defined by Eq. (2). The resonance frequencies in the modified BPM Button geometry, exhibit a much stronger dependence on the presence of the dielectric. The frequency of H_{110}-mode is f = 10.5 GHz for AlN (black curve) and f = 13 GHz for BN (red curve).

One of the possibilities from impedance optimization point of view is to increase the cutoff frequencies of the generated modes beyond the bunch spectrum. It can be done due to modification of the button geometry. The effect of the vacuum insulator on narrow band impedance needs to be taken into account. One of the solutions is to hide the vacuum insulator from the beam.

CANDIDATE GEOMETRIES

Three BPM Buttons have been designed and their first prototypes are under way. Several button geometries have been analysed. The process of choosing the three candidates (Fig. 3) was based on keeping the best two geometries (Bell-Shaped Button and Flat Button) from the electromagnetic analysis point of view and having the Step-Shaped one as a safe plan. The last one (Fig. 3b) is based on a well-known button geometry implemented at ALBA [5], just like the standard button geometry presented in Fig 1a. The Flat Button geometry (Fig. 3c) has been designed in a way to hide the vacuum insulator from the beam. The Bell-Shaped geometry (Fig. 3a) has a special form, which not only allows us to also hide the insulator, but to increase the button cut-off frequency (Eq. 2), without losing its sensitivity, since its bottom face area was kept the same as the other geometries.

The BPM Button diameter is taken to be 6 mm for all geometries to provide about 100 nm position resolution at 100 mA. This resolution considers a 15 dB noise figure (cables + electronics) integrated in a 2 kHz bandwidth.

The gap is 0.3 mm for each button. The instrumentation feedthroughs are designed for 50 Ω coaxial connectors: SMA, 3.5 or 2.4 mm types, to be defined.

The longitudinal narrow-band impedance is shown in Fig. 4. In the BPM Button geometries with BN insulator the lowest resonant modes exist at higher frequencies than in geometries with AlN. It agrees with the frequency dependence of the dielectric constant in Eq. (1). The frequency shift of the lowest mode is varied within 1-2 GHz for considered geometries. The lowest mode is the superposition of the electromagnetic fields in the gap and in the ceramics material.

As a conservative approach we can assume that the bunch length in the Sirius storage ring with passive third-harmonic Landau cavities will be extended at least by a factor of two, making all geometries as HOM's free ones.

The loss factor due to single bunch was calculated as a function of bunch length for all three geometries using the GdfidL simulated $ReZ_{||}(\omega)$ or $W_{||}(s)$. Summary results of κ_{loss} are shown in Table 2 for different σ_S. In the BPM Buttons design and in their optimization process, the results and experience at other synchrotron radiation facilities [6-8] were taken into account. As can be seen from Table 2 two new optimized BPM Buttons, Bell-Shaped and Flat, have the advantage over the standard Step-Shaped BPM Button at any σ_s.

ISBN 978-3-95450-127-4

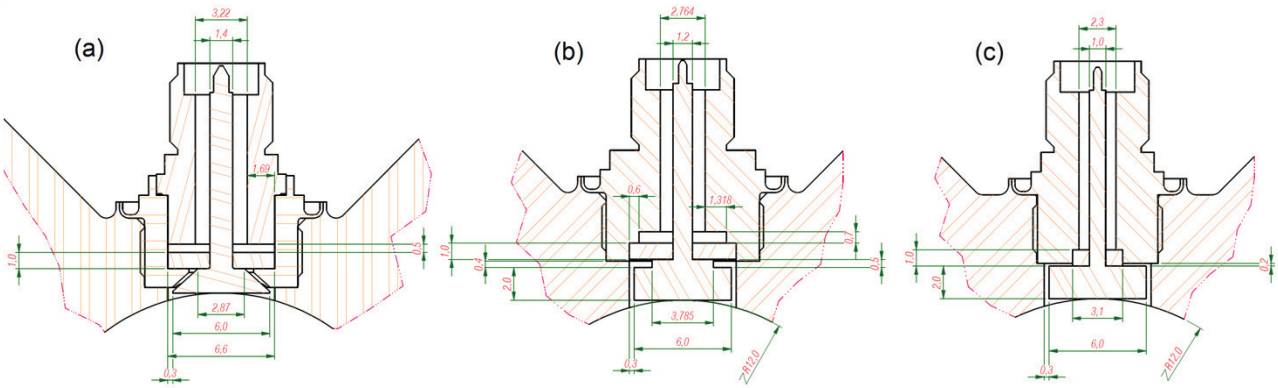

Figure 3: Engineering drawing of the BPM Buttons for: a) Bell-Shaped BPM Button. b) Step-Shaped BPM Button. c) Flat BPM Button.

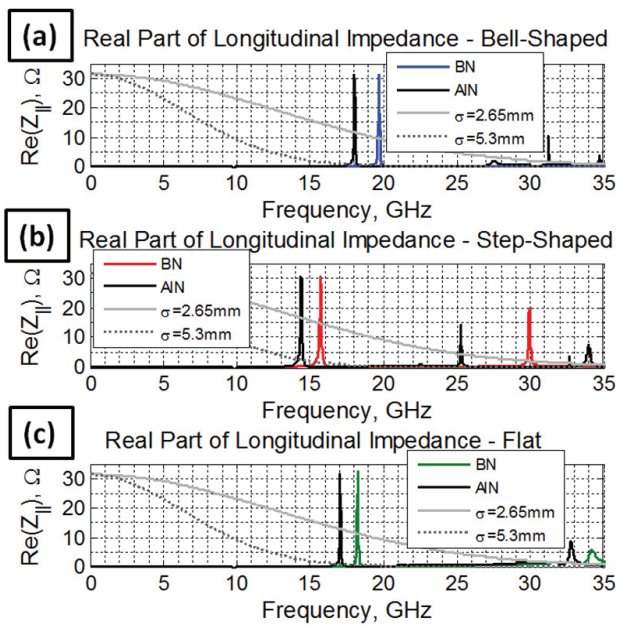

Figure 4: Real part of the longitudinal impedance for: a) Bell-Shaped BPM Button. b) Step-Shaped BPM Button. c) Flat BPM Button. Bunch profiles are in gray color for $\sigma_S = 2.65$ mm (solid) and $\sigma_S = 5.3$ mm (dotted).

The power loss goes from 1.9 to 4.4 W, for $\sigma_S = 2.65$ mm, at $I_{av} = 500$ mA in M = 864 bunches and 1.73 μs revolution period T_0.

$$P_{loss} = T_0 \frac{I_{av}^2}{M} \kappa_{loss}. \quad (3)$$

Table 2: Summary results of the loss factor for 2.65, 4.5, and 6 mm bunch lengths, for the BPM Button geometries including the ceramics materials, AlN and BN.

Geometry	κ_{loss}, mV/pC		
	Bell-Shaped	**Step-Shaped**	**Flat**
σ_S, mm	**2.65–4.5–6.0**	**2.65–4.5–6.0**	**2.65–4.5–6.0**
AlN	4.5–0.9–0.3	8.9–2.5–0.8	5.6–0.9–0.2
BN	3.6–0.8–0.4	8.3–2.3–0.7	4.6–0.7–0.2

MECHANICAL ASPECTS

The BPM Assembly of the Bell-Shaped button is shown in Fig. 5 in a perspective view:

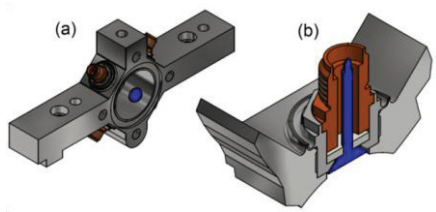

Figure 5: First Sirius BPM Prototype of the Bell-Shaped Button. a) BPM Assembly in the perspective view. b) One-half of the BPM Button located on the circular vacuum chamber (zoomed part).

Based on experience at other facilities [4], the coaxial cavity effect of the BPM Housing with the Body needs to be eliminated. The idea of using threads came up to obtain more benefits beyond the RF shielding: a better thermal contact between the housing and the body is required. After tightened with appropriated torque, the housing can be welded to the BPM body. However, it is well known that such threads can cause virtual leaks that can violate vacuum requirements. In order to reduce this problem, some valleys were designed to work as gassing channels, highlighted in Fig. 6.

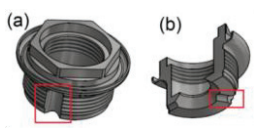

Figure 6: Housing of the Bell-Shaped Button, with highlighted gassing channels: a) Side channel. b) Bottom channel.

Other mechanical aspects are briefly discussed:

- Reverse polarity connectors: the button pin can be a male conductor, avoiding the need of BeCu spring fingers that can be easily damaged. The price is a drawback;
- Constant pin diameter: brings improvements in mechanical resistance and in the thermal contact area between the pin and the ceramics. Also it allows to have the button and the pin as a single piece;

ISBN 978-3-95450-127-4

- Tiny dimensions require very small tolerances and precise alignment. It makes the brazing process harder (small filler sites, short circuit risks, etc.);
- Materials choice: The higher the button electrical conductivity, the lower the button power dissipation [8]. Brazing and welding process play also a big role on materials choice;
- Vacuum insulation between the BPM body and housing: only test of the first prototypes will show the success of the welding. Flanges tightened by the housing outer threads can be used as an alternative. Several tests will be carried out to verify the required torque.

HEAT TRANSFER ANALYSIS

Due to thermo-mechanical aspects, the materials were initially chosen as: Stainless Steel (σ_t = 15.1 W/K.m) for the BPM Body, Kovar (σ_t =17.3 W/K.m) for the Housing and Molybdenum (σ_t = 138W/K.m) for the Button. The temperature of BPM body was specified 30 ºC for all three geometries, which is related to the nominal temperature of the Sirius vacuum chamber. Radiation heat transfer was ignored and air convection was set on respective surfaces. One Watt per button was applied to each bottom face as a worst-case scenario (Eq. 3).

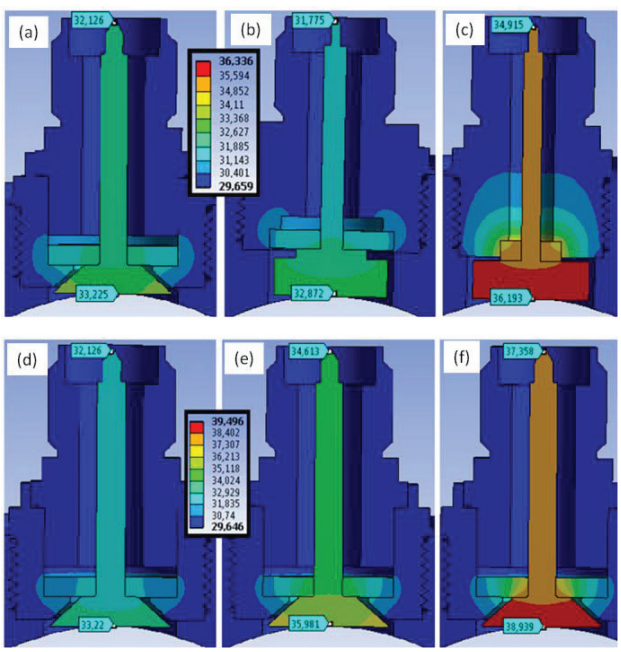

Figure 7: Thermostatic results for: a) Bell-Shaped BPM Button. b) Step-Shaped BPM Button. c) Flat BPM Button. AlN ceramics was considered as vacuum insulator (upper figure). Temperature profile of Bell-Shaped Button with: d) AlN. e) BN. f) Alumina 96% (lower figure).

The thermal behaviour the candidate geometries is shown in Figs. 7a-c. AlN ceramics is considered as the vacuum insulator. The Bell-Shaped geometry has been simulated for three different ceramics and the results can be seen in Figs. 7d-f. Alumina 96% (ε_r = 9.4, σ_t = 24 W/K.m) was added as extra material. This ceramics is strongly considered for prototyping phase, since the brazing technique of this ceramics is well know by the LNLS Materials Group.

The Step-Shaped Button has lower temperatures due higher contact area between the button and ceramics. All buttons have a temperature gradient (from bottom face to the top of the pin) of ~1.2 ºC. AlN ceramics drains more heat from the button due to its higher thermal conductivity. Button temperature gradient was of ~1.1 to 1.6 ºC.

CONCLUSIONS

Three different presented geometries of the BPM Button are good candidates for the Sirius storage ring. Their design, electromagnetic analysis and thermal analysis have been discussed as well as the mechanical aspects. The kind of design we choose one will be determined mainly by the entire construction process: machining, assembling, brazing and welding. The Bell-Shaped BPM Button and the Flat BPM Button have shown promising electromagnetic performance. However, these geometries require more effort in production than the standard design. The entire project is very challenging; many techniques still need to be improved. The first prototypes are underway.

ACKNOWLEDGMENT

First and foremost, we would like to thank our colleagues F. Rodrigues, O. Bagnato, R. Defavari, R. Seraphim and T. Rocha from the mechanics, materials and vacuum groups for their tremendous support. We also wish to express our sincere gratitude to G. Rehm (DIAMOND), A. Olmos (ALBA), R. Nagaoka (SOLEIL) and G. Kube (DESY) for the useful discussions.

REFERENCES

[1] N. Kurita, D. Martin, C.-K. Ng, S. Smith, T. Weiland, "Numerical Simulations of PEP-II Beam Position Monitor", SLAC-PUB-95-7006, September, 1995
[2] A. Blednykh, M.J. Ferreira, S. Krinsky "Impedance Calculations for the NSLS-II Storage Ring", Proceedings of PAC09, Vancouver, BC, Canada (2009)
[3] W. Bruns, GdfidL code; http://www.gdfidl.de
[4] A. Blednykh, "Wake Loss Simulations at NSLS-II", Mini-Workshop, Oxford University, England (2012); http://www.diamond.ac.uk/Home/Events/Past_events/Simulation-of-Power-Dissipation---Heating-from-Wake-Losses.html
[5] ALBA website, Storage Ring Blocks and Buttons; http://www.cells.es/Divisions/Accelerators/RF_Diagnostics/Diagnostics/OrbitPosition/BlocksAndButtons/SR/
[6] A. Olmos, T. Günzel, F. Pérez, "BPM Design for the ALBA Synchrotron", Proceedings of EPAC 2006, Edinburgh, Scotland (2006)
[7] R. Nagaoka, J.-C. Denard, M.-P. Level, "Recent Studies of Geometric and Resistive-Wall Impedance at SOLEIL", Proceedings of EPAC 2006, Edinburgh, Scotland (2006)
[8] I. Pinayev, A. Blednykh "Evaluation of Heat Dissipation in the BPM Buttons", Proceedings of PAC09, Vancouver, BC, Canada (2009)

ISBN 978-3-95450-127-4